Design, finite element analysis and energy assessment of a hinged speed bump energy harvester with an integrated wrong-way vehicle deterrent

Naushad Ali[a,b]

[a]School of Mechanical Engineering, Vellore Institute of Technology, Vellore, India (where the work was carried out)

[b]Present address: Luton, United Kingdom

Corresponding author: Naushad Ali, naushada43@gmail.com

Preprint note: This is a preprint and has not yet been peer reviewed. It has been submitted for publication in the International Journal of Ambient Energy.

Abstract

Speed bumps make vehicles lose energy, and many studies have proposed recovering some of it for street lighting. This paper describes a hinged speed bump harvester that drives three DC generators through a rack-and-pinion, gear and chain train, uses a two-stage variable pitch spring to give a full 80 mm stroke across vehicle masses, and carries cast iron spikes to deter wrong-way driving. Static finite element analysis showed that redesigning the bump geometry and supports cut peak deformation from 4.13 mm to 0.11 mm and peak stress from 484 MPa to 6.9 MPa. The spring reached 397 MPa under a 1500 kg vehicle, with a minimum factor of safety of 4.2. An energy balance shows that, with one 700 kg vehicle every 15 s, traffic supplies at most 0.88 kWh per day, or 36.6 W on average. Allowing for conversion losses, realistic output is 0.26–0.53 kWh per day, enough for one or two 24 W LED street lights for 12 h and far below an earlier estimate of 6.2 kWh per day. The estimated cost for three sections is Rs 69,561. A small prototype demonstrated the mechanism qualitatively.

Keywords: speed bump; energy harvesting; rack and pinion; variable pitch spring; finite element analysis; wrong-way driving

1. Introduction

Vehicles approaching a speed bump slow down and then do work on the road surface as they ride over it. On a conventional bump that energy is lost. If the bump is allowed to move under the wheel, part of the work done in pushing it down can be converted into electricity, and this idea has attracted a large number of designs and prototypes. Reviews of road energy harvesting group the available technologies into electromagnetic, piezoelectric, thermoelectric and photovoltaic systems and compare them by power output, cost and technology readiness (Wang, Jasim, and Chen 2018). For speed bumps specifically, Del Castillo-García et al. (2018) classified existing traffic energy harvesting devices and estimated the energy and cost of each technology. The mechanical conversion problem is similar to that in regenerative vehicle suspensions, where rack-and-pinion, ball-screw and linear electromagnetic dampers have all been studied (Abdelkareem et al. 2018).

Mechanical speed bump harvesters based on a rack and pinion with a gear train are common because they use cheap, familiar parts. Olugboji et al. (2015) designed such a mechanism for street lighting, and their prototype produced 6 V DC as a demonstration of the principle. Gholikhani et al. (2019) tested an electromagnetic speed bump under simulated traffic loading in the laboratory and reported a maximum average power of 3.21 mW. More recently, Orovwode et al. (2025) examined speed bumps as a source of electricity for street lighting at a university campus. A recurring weakness in this literature, especially in design studies, is that daily outputs are calculated from generator equations without being checked against the energy that passing traffic can actually supply. That check is central to the present paper.

Speed bumps are also a safety device, and in India driving on the wrong side of the road is a significant cause of death. In 2019 it accounted for 6.1% of the 151,113 people killed in road accidents in India (MoRTH 2020), which corresponds to roughly 9,200 deaths. One-way spike barriers are used at some car park entrances to stop vehicles entering in the wrong direction. This paper explores combining such a deterrent with an energy-harvesting bump.

The aims of the work were to: (i) design a three-section hinged speed bump harvester with a variable pitch return spring; (ii) evaluate the bump, spring and wrong-way spikes using finite element analysis; (iii) estimate the electrical output using an energy balance, and correct an overestimate made in an earlier version of this design; (iv) estimate the cost; and (v) build a small working prototype.

2. System design

2.1 Concept and mechanism

The bump is a half-cylindrical shell hinged along one edge, so that it swings down like a door when a wheel presses on it. Its overall dimensions are 4.17 m long, 0.684 m wide and 0.285 m high. The maximum rotation is 9°, which at the rack connection point, 506 mm from the hinge, gives a downward travel of about 80 mm. Rubber stops limit the travel to this value, and a shock absorber damps the motion.

A connecting rod links the underside of the bump to a vertical rack. The rack drives a pinion of 45 mm pitch radius. On the same shaft, a 260 mm gear drives a 100 mm gear, and a chain and sprocket stage carries the motion to a final pair of gears with 28 and 11 teeth, the smaller of which drives a DC generator. A variable pitch spring between the bump and a concrete support returns the bump after each wheel passes. The complete harvester consists of three identical sections placed side by side across the lane, each with its own spring and generator, sharing a single bump (Figure 1). The components were modelled in SolidWorks and

Autodesk Fusion 360, and a motion study of the assembly confirmed that the mechanism moved as intended.

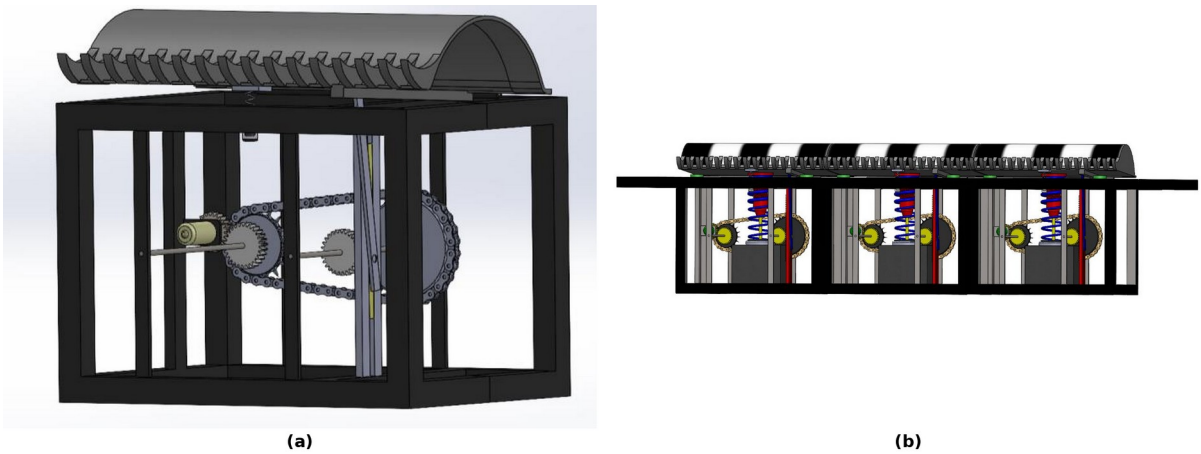


Figure 1. CAD model of the harvester: (a) a single section, showing the rack, gear train, chain drive and generator; (b) the three-section assembly with variable pitch springs.

2.2 Wrong-way deterrent

Cast iron spikes are fitted along the edge of the bump that faces traffic travelling in the wrong direction. The spikes are 34.7 mm long and spaced at 90.9 mm. Vehicles travelling in the correct direction approach the smooth face and push the bump down; a vehicle approaching from the other side meets the spikes first. Figure 2 compares the initial bump design with the final design, which includes the spikes.

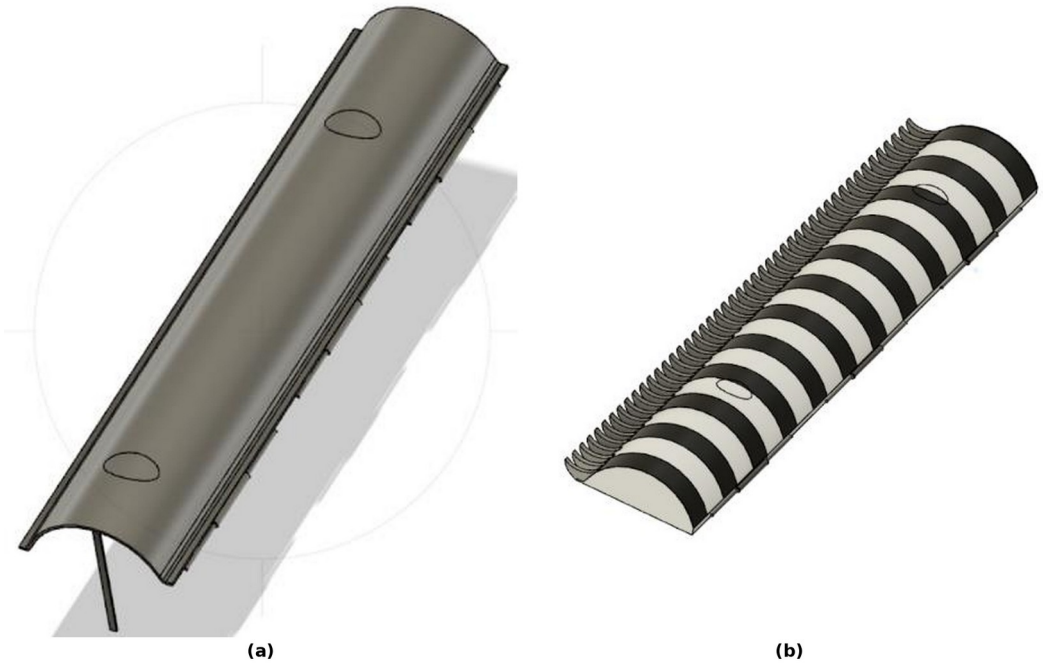


Figure 2. Bump designs: (a) initial model; (b) final model with wrong-way spikes along the leading edge.

2.3 Materials

Table 1 lists the materials chosen for the main components. The bump shell is PVC because it is the cheapest of the materials considered, with structural steel used for the hinges, where stresses are highest, and grey cast iron for the spikes. Material properties for the simulations were taken from the Ansys and Fusion 360 material libraries.

Table 1. Component materials in the final design.

Component	Material
Bump shell	PVC
Wrong-way spikes	Grey cast iron
Hinges	Structural steel
Base frame	Grey cast iron
Rack, gears and sprockets	Medium carbon steel
Chain	Medium alloy steel
Return springs	Low alloy steel
Spring support	Concrete
Travel stops	Rubber (70–80 Shore A)

3. Methods

3.1 Design loads

The bump was designed for a loaded compact sedan (Maruti Suzuki Swift Dzire) of total mass 1405 kg, with 60% of the weight on the front axle. The static front-axle load is therefore

$$F = 1405 \times 9.81 \times 0.6 = 8270 \text{ N} \qquad (1)$$

applied over the two front-tyre contact patches, each taken as an ellipse of 101.6 × 152.4 mm. Two further cases set the spring requirements: a light motorcycle of 162 kg including rider, with 52% of its weight on the front wheel (84.2 kg), and a light car of 1130 kg including four occupants, with a 60/40 weight distribution. Loads were treated as static; dynamic amplification from vehicles crossing at speed was not included.

3.2 Variable pitch spring

The spring must allow the full 80 mm stroke for light vehicles without being overloaded by heavy ones. For a 9° rotation, the deflection at the spring, 496.6 mm from the hinge, is 78 mm, rounded to 80 mm for design. The stiffness needed for the motorcycle case is 84.2 × 9.81 / 80 = 10.3 N/mm, shared between three springs, giving 3.44 N/mm per spring. For the light car the corresponding values are 6651 / 80 = 83.1 N/mm and 27.7 N/mm per spring.

The rate of a helical compression spring is (Budynas and Nisbett 2015)

$$k = G d^4 / (8 n D^3) \qquad (2)$$

where G is the shear modulus, d the wire diameter, D the mean coil diameter and n the number of active coils. With G = 81 GPa for low alloy steel and D = 139 mm, the soft section uses d = 9 mm, which requires n = 7.2 for 3.44 N/mm, and the stiff section uses d = 13 mm, which requires n = 3.9 for 27.7 N/mm. The two sections are wound as one spring of 396 mm free length, 198 mm per section. Under load the soft section closes first, so the effective stiffness rises with load.

3.3 Finite element analysis of the bump

Static structural analyses were carried out in Ansys R19.2. In the initial model all parts were structural steel. In the final model the shell was PVC, the hinges structural steel and the spikes grey cast iron, and the geometry of the shell and its supports was revised. Both models were meshed with adaptive tetrahedral elements. The load from Equation (1) was applied over the contact patches, and the hinge supports were fixed. Total deformation, von Mises stress, equivalent elastic strain and safety factor were evaluated. Ansys reports safety factors only up to 15, so only minimum values are meaningful.

3.4 Finite element analysis of the spring

The spring was analysed in Ansys with its base fixed and a force applied to its top plate, for vehicles of 100, 750 and 1500 kg. Each spring was taken to carry one third of the front-axle load:

$$F_s = m \times 9.81 \times 0.6 / 3 \qquad (3)$$

giving 196.2, 1471.5 and 2943 N. Wire diameter, coil diameter and number of coils were varied over 18 iterations before the final geometry was fixed.

3.5 Tyre impact simulation

To check whether the spikes would survive contact with a wrong-way vehicle, an event simulation was run in Fusion 360. The tyre was modelled as a ring of 381 mm outer diameter and 165 mm width, with steel beads, three steel belts, polyester plies and butadiene rubber; the tread pattern was omitted to keep the mesh manageable. The tyre rolled into the spikes at 10 m/s (ω = 52.5 rad/s) and the simulation covered 0.015 s. A real tyre of this width has an outer diameter of roughly 620 mm, so the model is a simplified representation of the impact rather than an accurate tyre model.

3.6 Energy assessment

The work a vehicle does on the bump sets an upper limit on the energy that can be harvested. If each axle pushes the bump down through the stroke s, the work done by a vehicle of mass m crossing the bump is

$$W = mgs \qquad (4)$$

since the axle loads together equal the vehicle weight. Traffic was assumed to be mixed, with vehicles from 100 to 1500 kg and a mean of 700 kg, and to arrive at one vehicle every 15 s, or 5,760 vehicles per day. The electrical output is the mechanical input multiplied by an overall conversion efficiency η, which covers friction in the hinge, rack, gears and chain, damping in the spring and shock absorber, and generator losses at low speed. Because these losses were not measured, η was varied from 0.3 to 0.6. Output was expressed as the number of LED street lights of 24, 36 and 50 W that could be run for 12 hours per day.

3.7 Cost estimate

Component masses were taken from the CAD models and multiplied by material prices from online suppliers in 2022. Manufacturing was allowed for by adding 20% to the material cost, and a DC generator at Rs 4,900 was added for each section.

4. Results

4.1 Bump

The initial all-steel bump was not adequate. Peak deformation was 4.13 mm at the edge of the shell, peak stress reached 484 MPa near the hinge, and the minimum safety factor was 0.18, meaning the hinge region would yield (Figure 3(a), (b); Table 2). The final design deformed by at most 0.11 mm, with a peak stress of 6.9 MPa and a minimum safety factor of 12.5

(Figure 3(c), (d)). Peak deformation fell by a factor of 38, peak stress by a factor of 70 and peak strain by a factor of 36.

The final shell is PVC, which is far less stiff than steel, so the improvement cannot be due to the material. It came from the revised shell geometry and the additional support provided by the hinges and frame in the final model. An intermediate model with PVC hinges deformed by about 25 mm at the hinges, which is why the hinges were changed to structural steel.

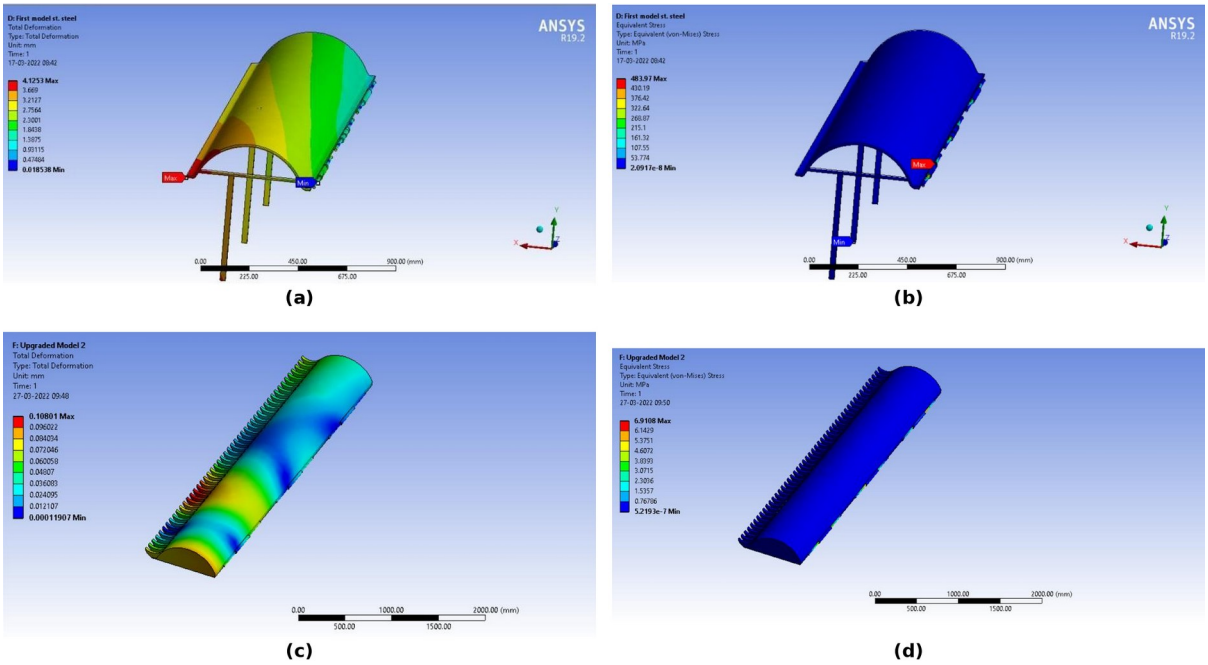


Figure 3. Static analysis of the bump: (a) total deformation and (b) von Mises stress of the initial steel model; (c) total deformation and (d) von Mises stress of the final model.

Table 2. Static finite element results for the initial and final bump models under the 8270 N front-axle load.

Model	Peak deformation (mm)	Peak von Mises stress (MPa)	Peak equivalent strain	Minimum safety factor
Initial (structural steel)	4.13	484.0	2.4×10^{-3}	0.18
Final (PVC shell, steel hinges, cast iron spikes)	0.11	6.9	6.7×10^{-5}	12.5

4.2 Spring

Table 3 summarises the spring results, and Figure 4 shows the 1500 kg case. The secant stiffness, the applied force divided by the peak deflection, rose from 2.07 N/mm at 100 kg to

12.4 N/mm at 750 kg and 20.7 N/mm at 1500 kg, confirming the progressive behaviour intended in Section 3.2. In every case the unrestrained deflection exceeded 80 mm, so in service the rubber stops would end the stroke at 80 mm and every vehicle class would drive the mechanism through its full travel. The highest stress was 397 MPa under the 1500 kg load, with a minimum safety factor of 4.2.

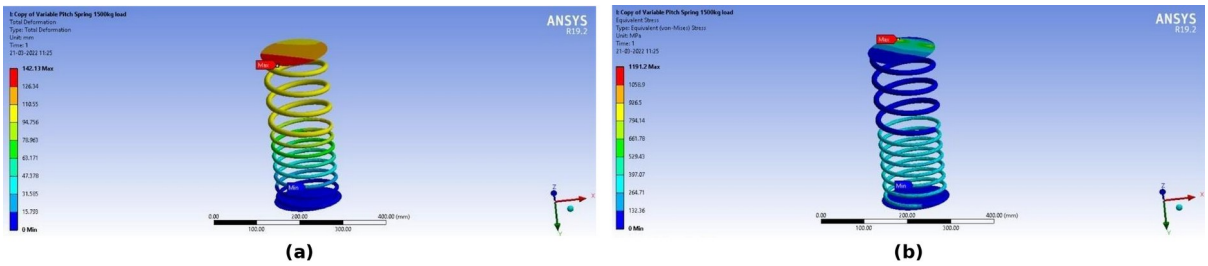


Figure 4. Variable pitch spring under the 1500 kg vehicle load: (a) total deformation; (b) von Mises stress.

Table 3. Finite element results for the variable pitch spring.

Vehicle mass (kg)	Force per spring (N)	Peak deflection (mm)	Secant stiffness (N/mm)	Peak von Mises stress (MPa)	Minimum safety factor
100	196.2	94.8	2.07	176.5	6.0
750	1471.5	118.4	12.4	220.6	5.0
1500	2943.0	142.1	20.7	397.1	4.2

4.3 Tyre impact on the spikes

At 0.015 s the tyre was deforming locally around the spikes, with a peak von Mises stress of about 28 MPa and equivalent strain of up to 0.90 in the rubber next to the spike tips (Figure 5). Stresses in the cast iron spikes remained low. The spikes therefore concentrate damaging stress in the tyre rather than in themselves, which is the intended behaviour. Whether this would cause a puncture or rupture in practice cannot be judged from this simplified model.

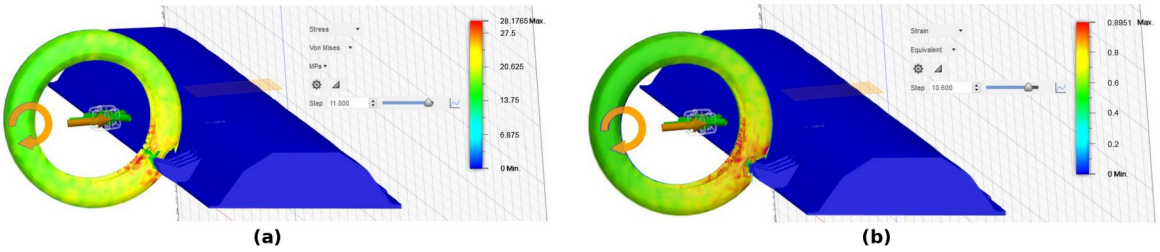


Figure 5. Tyre impact on the wrong-way spikes at 0.015 s: (a) von Mises stress; (b) equivalent strain.

4.4 Energy output

At the rack, the 9° rotation gives 79.5 mm of travel, which turns the 45 mm pitch-radius pinion through 0.28 revolutions. The 260/100 mm gear pair raises this to 0.73 revolutions and the 28/11 tooth pair to 1.86 revolutions of each generator per stroke. If the return stroke is also used, which would need one-way clutches or rectification because the rotation reverses, a two-axle vehicle turns each generator about 7.4 times.

Equation (4) gives an upper bound of 549 J for a 700 kg vehicle over an 80 mm stroke. At 5,760 vehicles per day this is 0.88 kWh per day, or an average mechanical input of 36.6 W. Table 4 shows the corresponding electrical output for the range of conversion efficiencies. At $\eta = 0.45$, the harvester delivers about 16.5 W on average and 0.40 kWh per day, enough for one or two 24 W LED street lights for 12 hours. Even if every joule of vehicle work were converted, it could run about three such lights.

Table 4. Estimated electrical output for one vehicle of 700 kg every 15 s (5,760 vehicles per day).

Conversion efficiency η	Average power (W)	Energy per day (kWh)	24 W lights for 12 h	36 W lights for 12 h	50 W lights for 12 h
1.0 (upper bound)	36.6	0.88	3.1	2.0	1.5
0.6	22.0	0.53	1.8	1.2	0.9
0.45	16.5	0.40	1.4	0.9	0.7
0.3	11.0	0.26	0.9	0.6	0.4

Number of lights = daily energy ÷ (lamp power × 12 h).

Figure 6 compares these figures with the estimate made earlier in this project, which put the DC output at 258.6 W continuously, or 6.21 kWh per day, enough for 21 lights of 24 W. That figure is 7.1 times the total mechanical energy that the assumed traffic can supply, so it cannot be achieved. The reasons are discussed in Section 5.1.

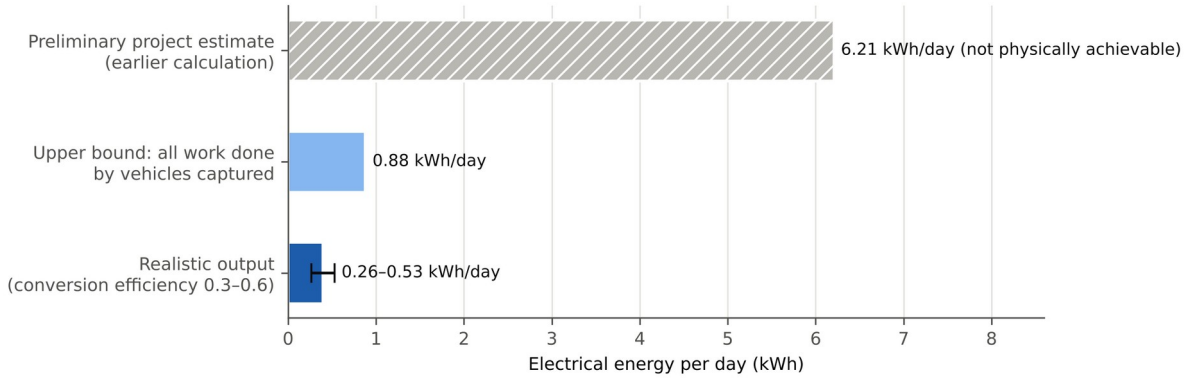


Figure 6. Daily electrical energy: the earlier project estimate compared with the upper bound set by the work done by vehicles, and the realistic range for conversion efficiencies of 0.3–0.6 (bar shows η = 0.45).

4.5 Cost

Table 5 gives the cost of one section. Materials cost Rs 15,239 and, with 20% added for manufacturing, Rs 18,287. Adding the generator gives Rs 23,187 per section and Rs 69,561 for the three-section harvester. At the mid-range output of 144 kWh per year, the capital cost is about Rs 482 per kWh of annual output, before installation, civil works and maintenance.

Table 5. Cost estimate for one section (2022 prices, Indian rupees).

Part	Mass (kg)	Material	Price (Rs/kg)	Material cost (Rs)	Including 20% manufacturing (Rs)
Spikes	41.545	Grey cast iron	45	1869.53	2243.43
Variable pitch spring	3.334	Low alloy steel	68	226.71	272.05
Hinges	4.165	Structural steel	75	312.38	374.85
Bump shell	101.955	PVC	100	10195.50	12234.60
Chain (inner links)	1.570	Medium alloy steel	54	84.78	101.74
Chain (outer links)	3.744	Medium alloy steel	54	202.18	242.61
Sprocket	2.818	Medium carbon steel	40	112.72	135.26
Outer gear	0.531	Medium carbon steel	40	21.24	25.49
Rack	1.461	Medium carbon steel	40	58.44	70.13
Pinion	0.980	Steel	68	66.64	79.97
Shaft 1	0.487	Steel	68	33.12	39.74
Shaft 2	0.487	Steel	68	33.12	39.74
Gear (inner)	0.980	Medium carbon steel	40	39.20	47.04
Gear (outer)	0.210	Medium carbon steel	40	8.40	10.08
Base frame	18.000	Grey cast iron	45	810.00	972.00
Shock absorber	17.134	Steel	68	1165.11	1398.13
Total				15,239.05	18,286.86

A DC generator (Rs 4,900) is added per section: Rs 23,187 per section, Rs 69,561 for three sections.

4.6 Prototype

A small-scale prototype was built from gears, sprockets, chain, springs and steel sections bought locally, with a welded steel frame and a bent steel sheet forming the bump (Figure 7). A small alternator was driven from the gear train and connected to a bulb. When the bump was pressed down by hand the bulb lit, confirming that the mechanism works as intended. No electrical measurements were taken, so the prototype demonstrates the principle only.

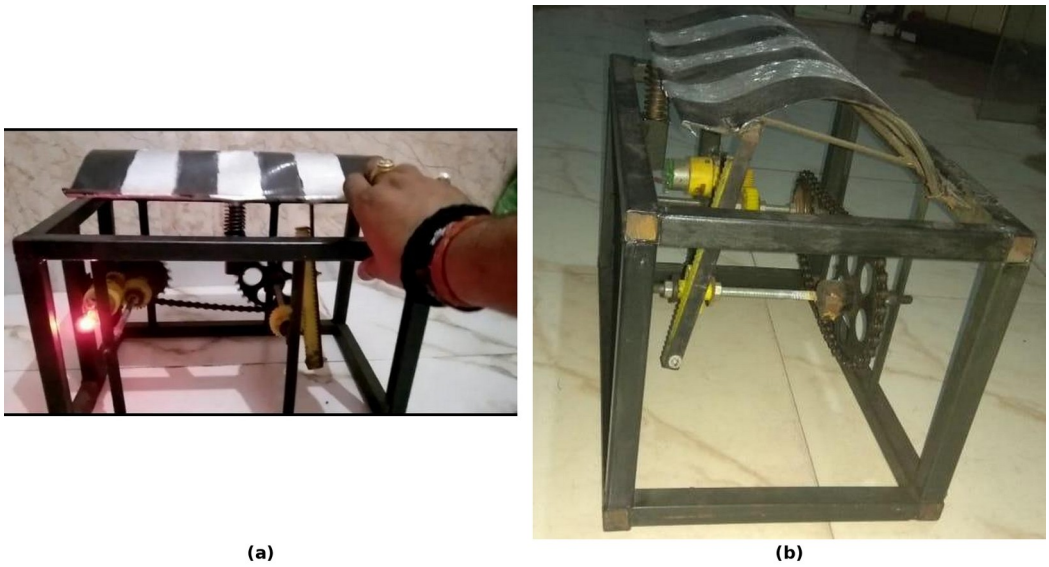


Figure 7. Prototype: (a) front view, with the bulb lit as the bump is pressed; (b) isometric view.

5. Discussion

5.1 Energy is the limiting factor

The main finding of this study is that the output of a mechanical speed bump harvester is limited by the energy traffic supplies, not by the size of the generator or the gear ratio. The earlier estimate for this design overstated the output for three reasons. First, the energy of one vehicle (549 J) was treated as if it arrived every second, while the traffic assumption was one vehicle every 15 s. Second, the generator EMF was calculated at a constant 96 rpm, which is the daily average speed, whereas the generator actually turns in short bursts as each axle crosses. Third, the use of three generators was taken to triple the output, although all three are

driven by the same vehicle work. In addition, the generator power was calculated as EMF × current, which includes the losses in the armature resistance; on the earlier assumptions only about 100 W of the 272 W would have reached the load.

The corrected output of a few hundred watt-hours per day is consistent with the modest outputs reported in prototype studies, such as the 6 V demonstration of Olugboji et al. (2015) and the milliwatt-level laboratory output of Gholikhani et al. (2019). A simple check against Equation (4) should be part of any speed bump harvester design, because generator equations alone can produce outputs that the traffic cannot supply.

5.2 Structural performance

The final bump has a large margin against static failure, but this depends on the revised geometry and supports rather than on PVC as a material. Before such a bump could be used on a road, its long-term behaviour would need to be assessed: PVC creeps under sustained load, is sensitive to temperature and ultraviolet exposure, and would be subject to millions of load cycles. The steel hinges carry the highest stresses and would be the critical parts for fatigue.

5.3 Wrong-way spikes

The impact simulation suggests that the spikes would survive tyre contact while concentrating stress in the tyre. However, spikes that damage tyres on a public road raise safety and legal issues that this study does not address. They could injure two-wheeler riders, hinder emergency vehicles that need to travel against the flow of traffic, and would require clear signage and approval from the highway authority.

5.4 Practical value

At about Rs 480 per kWh of annual output before installation and maintenance, the harvester is expensive as a source of electricity. Its value is more likely to lie in powering small local loads at the bump itself, such as warning lights, a single street light or traffic sensors, where running a cable would be costly, than in general street lighting.

6. Limitations

The loads were static and did not include the dynamic effect of vehicles crossing at speed. The tyre impact model used a simplified tyre smaller than a real one, without tread. The conversion efficiency was assumed rather than measured, and the prototype was tested qualitatively only, without electrical measurements. Traffic was represented by a single mean mass and a constant interval between vehicles. Fatigue, creep and environmental durability of the PVC shell and steel hinges were not analysed, and costs are 2022 material prices that exclude installation and maintenance.

7. Conclusions

A hinged, three-section speed bump harvester with a variable pitch return spring and wrong-way spikes was designed, analysed and demonstrated with a prototype. Revising the bump geometry and supports reduced peak stress from 484 MPa to 6.9 MPa under a loaded car, and the variable pitch spring allowed the full 80 mm stroke for vehicles from 100 kg to 1500 kg with a minimum safety factor of 4.2. An energy balance showed that, with one 700 kg vehicle every 15 s, traffic supplies at most 0.88 kWh per day and a realistic output is 0.26–0.53 kWh per day, enough for one or two 24 W LED street lights for 12 hours. This is about one-twelfth to one-twenty-fourth of an earlier estimate for the same design, which exceeded the energy available from traffic. Future work should measure the electrical output and conversion efficiency on a full-size prototype under real traffic, assess fatigue and durability, and examine the safety and regulatory implications of the wrong-way spikes.

Acknowledgements

This article is based on the author's BTech project at the School of Mechanical Engineering, Vellore Institute of Technology, supervised by Dr Srinivasan Narayanan. The author thanks Dr Sitharthan R for advice on the choice of generator. The author used Gemini, a generative AI tool, to check the calculations, restructure the project report into article form and edit the text. The author reviewed the content and takes full responsibility for the article.

Disclosure statement

No potential conflict of interest was reported by the author.

Funding

The author received no funding for this work.

Data availability statement

Recordings of the CAD motion analysis, simulations and prototype testing are available at https://www.youtube.com/watch?v=7XnGMXfIooQ&list=PLEnaJfTLUfgp1DCxWt4U1Z9H46nODOgDf. The energy calculations are fully described in Section 3.6, and the other data supporting the findings are available from the author on request.

References

Abdelkareem, Mohamed A. A., Lin Xu, Mohamed Kamal Ahmed Ali, Ahmed Elagouz, Jia Mi, Sijing Guo, Yilun Liu, and Lei Zuo. 2018. "Vibration Energy Harvesting in Automotive Suspension System: A Detailed Review." *Applied Energy* 229: 672–699. https://doi.org/10.1016/j.apenergy.2018.08.030.

Budynas, Richard G., and J. Keith Nisbett. 2015. *Shigley's Mechanical Engineering Design*. 10th ed. New York: McGraw-Hill Education.

Del Castillo-García, Gonzalo, Elena Blanco-Fernandez, Pablo Pascual-Muñoz, and Daniel Castro-Fresno. 2018. “Energy Harvesting from Vehicular Traffic over Speed Bumps: A Review.” *Proceedings of the Institution of Civil Engineers – Energy* 171 (2): 58–69. https://doi.org/10.1680/jener.17.00008.

Gholikhani, Mohammadreza, Reza Nasouri, Seyed Amid Tahami, Sarah Legette, Samer Dessouky, and Arturo Montoya. 2019. “Harvesting Kinetic Energy from Roadway Pavement through an Electromagnetic Speed Bump.” *Applied Energy* 250: 503–511. https://doi.org/10.1016/j.apenergy.2019.05.060.

MoRTH (Ministry of Road Transport and Highways). 2020. *Road Accidents in India 2019*. New Delhi: Government of India, Transport Research Wing.

Olugboji, O. A., M. S. Abolarin, I. E. Ohiemi, and K. C. Ajani. 2015. “Modelling and Design of an Auto Street Light Generation Speed Breaker Mechanism.” *American Journal of Mechanical Engineering* 3 (3): 84–92. https://doi.org/10.12691/ajme-3-3-3.

Orovwode, H. E., J. A. Abubakar, O. O. Josiah, and A. Abdullkareem. 2025. “Harnessing Speed Breakers Potentials for Electricity Generation: A Case Study of Covenant University.” *International Journal of Electrical and Computer Engineering* 15 (3): 2669–2680. https://doi.org/10.11591/ijece.v15i3.pp2669-2680.

Wang, Hao, Abbas Jasim, and Xiaodan Chen. 2018. “Energy Harvesting Technologies in Roadway and Bridge for Different Applications – A Comprehensive Review.” *Applied Energy* 212: 1083–1094. https://doi.org/10.1016/j.apenergy.2017.12.125.